Physics-based description of gas breakdown

2007 J. Phys. A: Math. Theor. 40 1153

(http://iopscience.iop.org/1751-8121/40/5/019)

INSTITUTE OF PHYSICS PUBLISHING JOURNAL OF PHYSICS A: MATHEMATICAL AND THEORETICAL

J. Phys. A: Math. Theor. **40** (2007) 1153–1169 doi:10.1088/1751-8113/40/5/019

Physics-based description of gas breakdown

W N G Hitchon and C Wichaidit

Department of Electrical and Computer Engineering, University of Wisconsin, Madison, WI 53706, USA

E-mail: hitchon@engr.wisc.edu and wichaidi@cae.wisc.edu

Received 7 July 2006, in final form 16 November 2006
Published 17 January 2007
Online at stacks.iop.org/JPhysA/40/1153

Abstract

This paper develops an efficient method for simulation of breakdown in a gas, which explicitly makes use of the real underlying physics, in a case where standard numerical schemes are likely to fail. We develop a 'time-dependent capacitor model' (TDCM) for 2D or 3D, which ensures that the ionization rate is consistent with energy conservation and which disallows almost all numerical diffusion (and hence allows larger $(\Delta x, \Delta t)$). To avoid spurious ionization in the TDCM, density is only added in a cell when the density and electric field are high enough so that the density could physically grow to the expected final density within the cell. Numerical diffusion is negligible in the TDCM, in part because we only inject density into cells/capacitors when enough time has elapsed for density to be physically present. The direction of injection is controlled, so if, for example, density from cell $[i, j]$ in reality moves to cell $[i \pm 1, j \pm 1]$, it goes there directly, giving a physically correct direction of propagation. A simple scheme for accelerating convergence, exploiting the very different time scales which arise, is also discussed.

PACS numbers: 02.70.−c, 52.25.−b, 51.50.+v, 52.65.−y, 52.80.−s

1. Introduction

This paper is concerned with developing a physics-based approach to modelling a physical phenomenon, for which standard numerical methods fail. Breakdown in a dielectric barrier discharge (DBD) (or similar 'atmospheric-pressure' systems) is the critical phase of the discharge, in the sense that the processes that control the energy input and the formation of new chemical species tend to occur during breakdown. Breakdown has been modelled in a variety of ways. The extreme nature of breakdown, with density growing very rapidly in both space and time, makes this a very difficult phenomenon to describe numerically, however. Standard numerical schemes often fail to reproduce correct physics, and numerical errors can dominate over real physical behaviours. For these reasons, it is imperative to design models

which truly capture the behaviours which are believed to be present in reality. This is the main aim of this paper.

Numerical simulations suffer from a number of common pitfalls, some of which are discussed in [4, 5]. It can be very difficult to be sure that a simulation is accurate and believable. The types of errors which must be considered range from undiscovered errors in logic, through the use of numerical schemes with behaviours which are purely artefacts of the scheme, to employment of physical models which are inappropriate in some parameter ranges. Partly for these reasons, some computational physicists place great emphasis on examining the results of their simulations to make sure they can be explained with simple physical reasoning; if they cannot, it is considerably more difficult to be confident in the results [24].

We have previously developed methods to solve the Boltzman equation which explicitly incorporate the pertinent physics [5]. In this paper, we adopt a similar approach to describing breakdown of a gas. Firstly, we set up a computational model which is designed to explicitly exhibit a specific, rather straightforward set of physical behaviours. This is the main focus of this paper. Our goal is, at least in part, to argue and illustrate that simulation should be based on physical considerations. Secondly, the discussion of results will reflect a physical analysis which is designed to confirm that the findings are indeed plausible. Since our emphasis is primarily on the method of simulation, we do not go into great detail in discussing the physics.

The available numerical schemes can be divided into those which use a single fluid equation to describe the electrons (that stating particle conservation), relying on equilibrium assumptions to close the system, and those which use more moments—in particular, those which employ the energy conservation equation in addition. The equilibrium fluid equations can exhibit spurious ionization and this leads to significant errors [2]. The errors in an equilibrium model occur both early during breakdown when the electric field is very strong and later on when the electric field starts to be shielded out. When the field is strong, the equilibrium model overestimates the ionization rate on the upstream side of the plasma and gives the same overestimate over a wide range of discreteness parameters $(\Delta x, \Delta t)$. This means that the effect is not rectifiable by reducing numerical diffusion by means of a flux-conserving scheme. When we turn to an energy-conserving scheme we find that it is not subject to this problem of spurious ionization. Strictly speaking, in the energy-conserving scheme spurious ionization is modest in general and negligible provided we employ rather small discreteness parameters. The limitations on $(\Delta x, \Delta t)$ can be partially overcome by using a propagator (i.e. Lagrangian) scheme that also allows the density to grow exponentially with the gain in energy as particles move from cell to cell [2, 3]. All of these schemes are subject to numerical diffusion to varying degrees, however, and this can be a severe problem in breakdown simulations.

The capacitor model which we introduce here provides a physically based description of breakdown. It divides the plasma into isolated 'capacitors', reflecting the fact that the time scale for density growth during breakdown is much shorter than transport time scales. This is probably the central physical assumption of the present work. Once density is introduced to a region with a strong electric field, breakdown is very fast. The capacitor model reflects this by only allowing density to be introduced into capacitors at the physically correct times (as discussed in detail below.) This procedure essentially prevents numerical diffusion and similar errors. It introduces a second type of error however; since each capacitor is physically isolated, it is difficult to employ energy conservation in a fully consistent form. An energy-conserving version of the scheme, which partially relaxes the isolation of capacitors, is outlined in the appendix. Spurious ionization is avoided by only introducing density into capacitors where

and when that density could physically grow to the level encountered after breakdown. The main advantages of the capacitor model are its speed and accuracy—especially its ability to control numerical diffusion, including diffusion which obscures the direction in which breakdown proceeds.

The time scale for density growth during breakdown is $\tau_G \lesssim 10^{-10}$ s; the transport time scale (for a distance $L \sim 10^{-3}$ m) during breakdown is $\tau_{tb} \gtrsim 10^{-8}$ s; the transport time scale in the plasma, τ_{tp}, depends on the electron temperature, which falls rapidly, but $\tau_{tp} \gtrsim 10^{-3}$ s. The first two of these imply a severe restriction on the mesh size, in any scheme which exhibits numerical diffusion [2]. The introduction of density into cells where it physically could not or should not be is what we generally mean by numerical diffusion. In most mesh-based schemes which are used to describe transport, we tolerate numerical diffusion and rely on the vast majority of particles being in the right place. The fact that the outliers behave unphysically is overlooked because their numbers are generally low. In problems such as ion implantation the outliers are critical [23] but in general this is probably not the case. Breakdown is a situation where outliers are critical — because even a small density can grow to a very large value, and this can happen very quickly because $\tau_G \ll \tau_{tb}$. Introduction of spurious density into a cell which should be empty leads to a chain reaction of growth and spreading of density into other cells which should also be empty. Numerical diffusion can be limited by use of a flux-corrected transport (FCT) scheme [16–18], although we argue here and elsewhere that this is not sufficient to remedy the equilibrium fluid equations.

The issues which drive the work of this paper are summarized by saying that we wish to ensure the physics is preserved, and to do this we limit numerical diffusion by only allowing particles to move from cell to cell in a controlled set of circumstances. In order to move particles only where they should physically go, and to make sure that energy conservation is built into our scheme, we 'inject' particles into cells according to a set of rules. These points (and the rules of injection) will be explained in more detail in section 3. Finally, a scheme is presented to speed up the simulation, which exploits the fact that drift times are much longer than the time scale for density growth.

In the previous work, we described a number of issues which cause complications in one-dimensional modelling. The advantages and disadvantages of the available schemes were discussed [1]. We recap these points briefly below. Needless to say, there are more difficulties in higher dimensions, and these are a large part of what we address here.

2. Capacitor model

The 2D time-dependent capacitor model (TDCM) is a simple physical model of breakdown and is largely based on the same principles as the 1D TDCM which was described elsewhere [1]. The two-dimensional discharge (excluding the dielectric slabs and electrodes) in Cartesian coordinates is divided into a total number of nodes N with separations of Δx and Δy in the x- and y-directions. ($N = N_x \times N_y$; N_x is the number of nodes in the x-direction, N_y is the number of nodes in the y-direction.) There is no reason in principle for a Cartesian mesh, but for the present it is convenient. The discharge consists of a total number of N_c small capacitors, where $N_c = (N_x - 1)N_y + (N_y - 1)N_x$. (Different sizes of capacitors can be used. In this work, all the capacitors which lie in the same direction have the same capacitance. The capacitance of each capacitor in the x-direction is not equal to those in y; $\Delta x \neq \Delta y$.) A number of electrons N_e is placed at each node (i.e. $N_e[k]$ denotes a number of electrons at node k, where k is a function of $[i, j]$). Each capacitor is placed between a pair of nodes (shown in figure 1). The total charge at each node is calculated by summing all of the charge

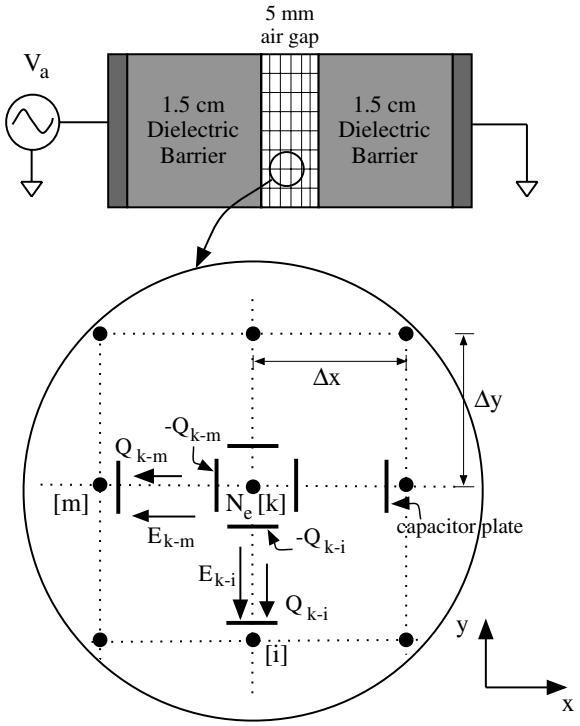

Figure 1. Schematic illustrates a network of capacitors in an air gap and shows how charges Q_{k-m} and Q_{k-i} move between nodes k and m, and k and i, due to the electric fields $\boldsymbol{E}_{k-m}$ and $\boldsymbol{E}_{k-i}$ respectively, during a time step.

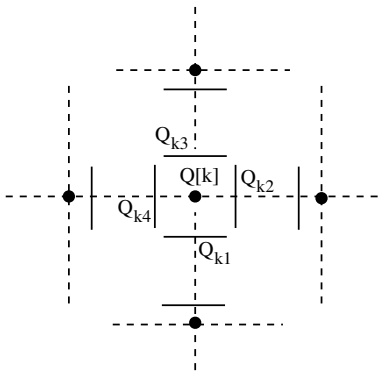

Figure 2. Schematic illustrates charges placed on the capacitor plates at node k. The total charge $Q[k]$ at node k equals $\sum_{i=1}^{4} (\mathrm{Q}_k)_i$.

on each capacitor 'plate' around that node. As shown in figure 2, for instance, the total charge at node k is obtained from

$$Q[k] = Q_{k1} + Q_{k2} + Q_{k3} + Q_{k4}. \tag{1}$$

The voltage at each node is calculated using the Green's function $G[k, s]$ (which was precalculated using SGFramework [4]), e.g. the voltage at node k is

$$V[k] = \sum_{s=1}^{N} G[k, s]Q[s]. \tag{2}$$

During a time step, some fraction of the density is allowed to move within a capacitor (or, in another words, between a node and one of its neighbours), resulting in a charge moving to a capacitor 'plate'. For example, when an iteration runs over the capacitor between node k and node m (denoted as C_{km}), the amount of charge

$$Q_{k-m} = \frac{N_e[k]}{\Delta x}\,\mu\,\boldsymbol{E}_{k-m}\,\Delta t, \tag{3}$$

where $\mu \equiv \mu(E_{k-m})$ moves from node k to a capacitor plate of node m as shown in figure 1. Here $\boldsymbol{E}_{k-m}$ is the electric field between nodes k and m, assumed to be in the direction towards node m, and μ is the (electron) mobility which corresponds to E_{k-m}. (This mobility is negative.) At the same time, an equal and opposite amount of charge $-Q_{k-m}$ is put on the other capacitor 'plate' of capacitor C_{km} (the capacitor plate of node k which is paired up with a plate at node m).

The energy, W, expended in each capacitor is calculated from the change in potential energy, which is the force (due to the electric field) multiplied by the distance that particles move, e.g. W_{k-m} delivered to the capacitor between nodes k and m is found from

$$\begin{aligned} W_{k-m} &= -Q_{k-m}\boldsymbol{E}_{k-m}\Delta x \\ &= Q_{k-m}V_{k-m}, \end{aligned} \tag{4}$$

where V_{k-m} is the voltage difference between nodes k and m. Consequently, the number of electrons, $\Delta N_e[k]$, and ions, $\Delta N_i[k]$, which are created at node k by electrons moving from node m to node k and the associated ionization process (as opposed to the energy going into excitation and other processes) are determined from

$$\Delta N_e[k] = \Delta N_i[k] = \frac{\alpha W_{k-m}}{\mathcal{E}_{\mathrm{iz}}}. \tag{5}$$

Here $\alpha \equiv \alpha(E_{k-m})$ is the fraction of the energy that goes into ionization, as a function of the electric field between nodes k and m, and $\mathcal{E}_{\mathrm{iz}}$ is the ionization potential. These newly created particles are put back at node k to avoid any unwanted numerical diffusion and to conserve the locality of the scheme. Particle transport between capacitors, referred to as 'seeding of electrons' or 'density injection', only happens when it is explicitly allowed to. Once the density and charge at each node are all, in turn, updated, the voltage and the electric field in the discharge will then be updated.

During the breakdown, the electric field in each capacitor will tend to be reduced due to the increase of the surface charge on the capacitor plates. Similarly to the 1D TDCM, the breakdown in each capacitor is complete when, for instance, $|\boldsymbol{E}_{k-m}|$ falls so as to be equal to or below a preset value. However, instead of replacing the broken-down capacitor with a short circuit (as in the 1D TDCM) and to be more realistic in 2D, the particles in that capacitor are still allowed to move (from one 'plate' to another) according to the value of the instantaneous electric field. We note that, if the capacitors are completely isolated, shielding must be achieved within one capacitor, so if its final electron density is n_e and its width is Δx, the maximum field it can shield is

$$E_s = q n_e \frac{\Delta x}{\varepsilon}. \tag{6}$$

Sine n_e depends on E^2, this puts a lower limit on E or a lower limit on Δx.

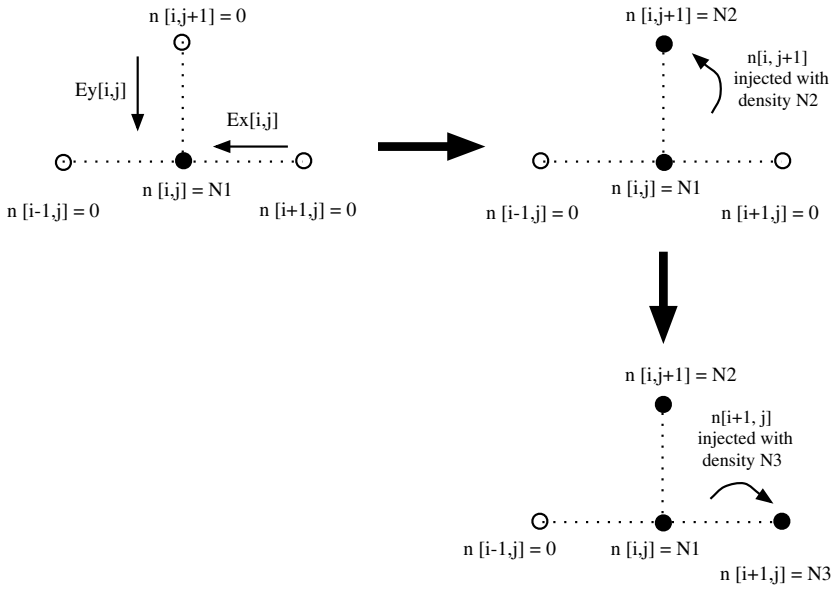

Figure 3. Schematic illustrates the spurious effects which occur when the numerical movement of particles is along the axes. Node $[i, j + 1]$ acquires density N_2 injected from node $[i, j]$, and similarly node $[i + 1, j]$ acquires density N_3 from node $[i, j]$. In this case, numerical diffusion is introduced along the axes; the real density movement should have fallen diagonally between the x and y axes.

3. Energy conservation and density injection

We now turn to the issues which determine when density is first introduced into a cell. The main concerns are that transport into a cell should be at the correct time, that transport should be in the correct direction and that cells where the density cannot grow significantly according to energy conservation should not exhibit breakdown. The final density which can be produced in a cell is (approximately) the initial density in the cell multiplied by $e^{(\alpha\delta\mathcal{E}_i/\mathcal{E}_{iz})}$, where $\delta\mathcal{E}_i$ is the potential energy dropped across cell i. If this product is too small to shield out the electric field, the initial density is said to be below 'threshold' and injection is not allowed to take place. Two forms of injection have been found to be necessary, depending on whether the density threshold limit can prevent injection or not; these are described in more detail below.

The direction of injection is critical for preventing a significantly troublesome form of numerical diffusion. If injection is along the coordinate axes, as transport inevitably will be in most finite difference schemes (but unlike a propagator scheme [3]) then density will spread along the axes, even in situations where the actual movement should fall between the axes. Suppose E_x and E_y are both nonzero. The direction of injection should be given by

$$\frac{\delta y}{\delta x} = \frac{E_y}{E_x}, \tag{7}$$

where δx and δy are distances that density moves in the x- and y-directions. It is possible to make the injection be in a diagonal direction, instead of injecting in two separate directions—one in x and one in y. Figure 3 illustrates the (usual) case where the injection is implemented (incorrectly) so that particles drift along the x and y axes separately. A group of electrons drifts from cell $[i, j]$ to $[i, j + 1]$. Similarly node $[i + 1, j]$ gets injected with density. Therefore, cells $[i, j + 1]$ and $[i + 1, j]$ have nonzero densities. Yet neither cell should have density in it.

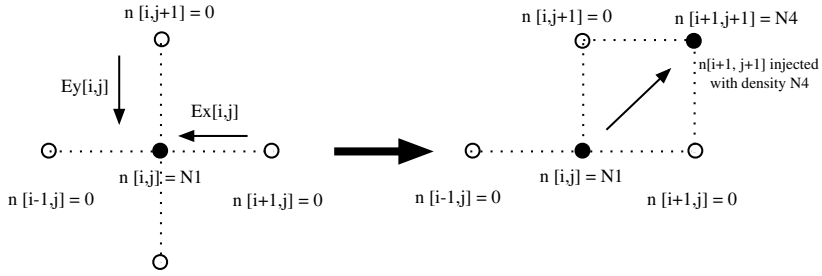

Figure 4. Schematic illustrates how, e.g., cell $[i+1,\ j+1]$ is injected with particles from cell $[i,\ j]$, allowing for the effect of both E_y and E_x at cell $[i,\ j]$. In other words, injection is done in the cell nearest to the physically correct trajectory, without going through intermediate cells which are not on the trajectory.

This type of injection introduces numerical diffusion. Especially in the breakdown process, if the density is initially misplaced, a small seeded density can lead to a great deal of artificial growth.

We now discuss one way to implement the injection more accurately. Other approaches would clearly also be possible. In the time particles move Δy in y, instead of injecting a group of particles to cell $[i,\ j+1]$ (as explained above and in figure 3), which implies $\delta x = 0$, that group of particles should move a distance

$$\delta x = \frac{E_x}{E_y}\Delta y \tag{8}$$

in x. The nearest cell in x is employed, in the simplest possible approximation. If $1.5\Delta x > \delta x > 0.5\Delta x$, then that group of particles should be injected into the next adjacent cell in x. Thus, instead of injecting into $[i,\ j+1]$ we should inject into $[i+1,\ j+1]$, assuming we are moving from bottom left to top right as shown in figure 4. (We calculate the time for particles to move a distance Δy and at that time inject particles at $y + \Delta y$ and the nearest cell in x. We also calculate the time to move Δx, and inject at $x + \Delta x$ and the nearest cell in y. This allows injection to several cells close to the true trajectory, see figure 5.) If $\left|\frac{\delta x}{\Delta x}\right|$ or $\left|\frac{\delta y}{\Delta y}\right| > 1$, then it is necessary to make sure that the movement all along the path to the final cell is energetically allowed. The motion will be truncated otherwise. As mentioned above, in the case of breakdown we cannot rely on the density being small in outlying regions—breakdown will likely lead to the density very rapidly becoming high wherever any density at all is introduced.

It was convenient to construct an array $t_{\min}(i)$ where i refers to the cell into which injection occurs and $t_{\min}$ is the earliest time of injection from all sources. Any given cell which acts as a source of density can inject into many other cells, at different times, as the fields evolve. A cell which is being injected into need only be labelled by the first time $t_{\min}$ when it receives density, although $t_{\min}$ also can vary as the run progresses.

The next two sections discuss threshold and drift injection in quantitative terms.

3.1. Threshold density injection

Suppose the distance for an electron to produce another electron is l_d:

$$l_d = \frac{\mathcal{E}_{\text{iz}}}{qE\alpha}. \tag{9}$$

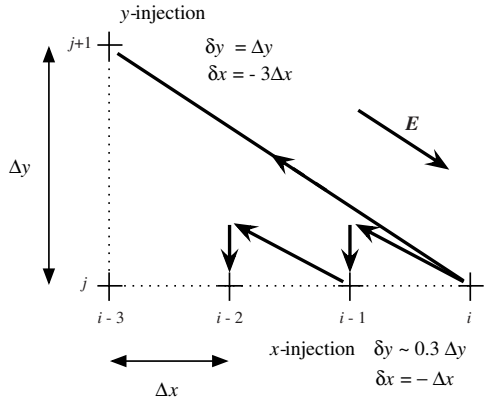

Figure 5. Schematic shows an example of injection in the x- and y-directions for a particular electric field $\boldsymbol{E}$. In y-injection, the electrons are injected from cell $[i, j]$ to the cell closest to their actual trajectory after moving through one cell width in the y-direction, which in this case is $[i-3, j+1]$. In x-injection, the electrons are injected, e.g., from cell $[i, j]$ to $[i-1, j]$ which is the closest cell to their trajectory after they move through Δx in the x-direction.

l_d is about 10–40 μm for our conditions. A single electron will produce 10^{12} electrons in 40 l_d; and if 40 l_d is smaller than a capacitor size, the breakdown will almost certainly still appear microscopic, i.e. local, within a cell. The initial density must be within a certain range, depending on l_d and the cell width, to be able to grow to reach saturation within the width of the cell. If the initial density is not in that range, then it is allowed to travel downstream until it has gone far enough that it is in the range, and then we inject density in the cell(s) where the density reaches a level which is high enough; $n_e \gtrsim n_{\rm th}$, where $n_{\rm th}$ is threshold density.

In our examples, we estimate that the cell width $\Delta x \sim 15 l_d$, so the density can rise by a factor up to 3×10^4 while crossing the cell. A final density of $n_f \simeq 10^{13}$ cm^{-3} in a given cell could be produced by an initial density less than $n_{\rm th} \gtrsim 10^9$ cm^{-3} which started in the same cell. An initial density of less than about 3×10^8 cm^{-3} will contribute less than n_f within the same cell where it started.

The density which initially seeds the discharge is denoted by n_s. This density needs to double N_s times before it reaches threshold, and will go a distance $N_s l_d$, before it reaches a cell where it makes a significant contribution to the final density; in that cell its density will reach $n_{\rm th}$. Thus, the initial density n_s leads to injection of a density $n_{\rm th}$, a distance $N_s l_d$ downstream, after a time delay

$$t_{\rm th} = \frac{N_s l_d}{v_{\rm dr}} \tag{10}$$

where $v_{\rm dr}$ is the drift velocity. Any capacitor that has density less than the threshold density is not allowed to start breaking down unless it gets injected from somewhere else.

Let the maximum fractional growth of n_e within a cell, for any given electric field, be g_c. If n_f is the approximate final electron density after the capacitor has broken down, then if a capacitor is to break down, its initial density must be $\geqslant n_{\rm th} = \frac{n_f}{g_c}$. In figure 6, capacitor k initially has density higher than $n_{\rm th}$; while capacitor $k+1$ does not. When the run starts, capacitor k is allowed to start breaking down. Figure 6 shows that the numbers of particles from capacitor $k+1$ grow exponentially as they cross capacitor $k+2$ and reach a density $n_e \gtrsim n_{\rm th}$ in capacitor $k+3$. Thus, capacitor $k+3$ gets injected with the determined density $n_e \gtrsim n_{\rm th}$ at time $t_{\rm th}$, and then breakdown starts (in capacitor $k+3$). The initial density in

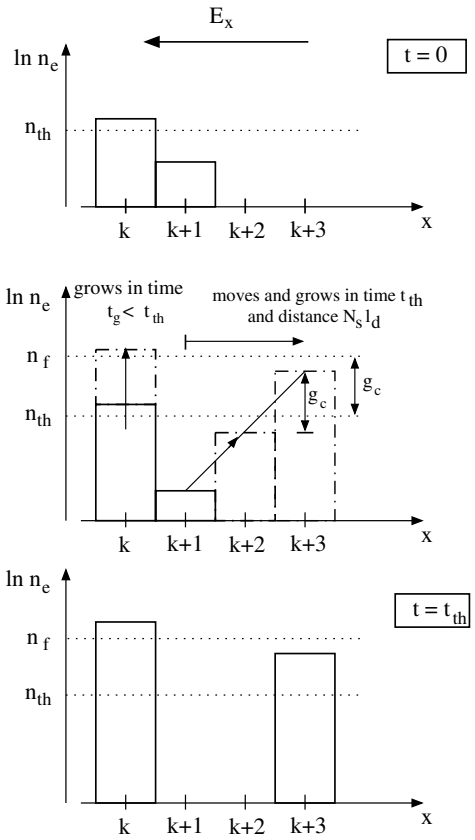

Figure 6. When the density in capacitor $k + 1$ is initially less than the threshold density, then particles in that capacitor have to move downstream in order to gain energy and grow in number such that their density reaches the threshold and breakdown can occur—in this case, in capacitor $k + 3$ (after travelling a distance $N_s l_d$ after a time delay $t_{\rm th}$). g_c is the maximum increase in density after crossing one capacitor. The original density in capacitor $k + 1$ is removed.

capacitor $k + 1$ is then removed. This threshold injection process occurs during the beginning of the breakdown (when the electric field is in its maximum range); thus, it is necessary to apply the exponential growth during the move. Since $n_e[k] \gtrsim n_{\rm th}$, the density in cell k will quickly reach its final value, and E_k in capacitor k will be shielded out. Since the field E_k in capacitor k is then relatively very small indeed, some density from capacitor k may be injected into capacitors downstream, but capacitor k is not expected to empty out again.

3.2. Drift injection

To illustrate drift injection using the previous example, particles with density well above threshold will drift out of capacitor k and 'inject' into $k + 1$ (if allowed by the electric field) in the time particles take to drift the distance Δx:

$$t_{\rm dr} \simeq \frac{\Delta x}{|\mu(E_k)E_k|}. \tag{11}$$

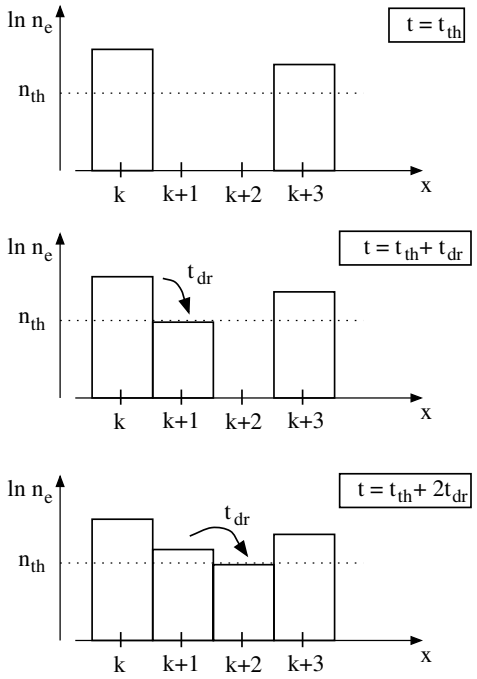

Figure 7. When $n_e[k] \gtrsim n_{\rm th}$, a density above threshold will move to $k+1$ in $t_{\rm dr} = \frac{\Delta x}{v_{\rm dr}}$, so density from capacitor k gets injected downstream in $k+1$ after a delay of $t_{\rm dr}$. Similarly for the injection from capacitor $k+1$ to $k+2$.

Similarly, after capacitor $k+1$ has been injected, then capacitor $k+2$ can be injected (either from capacitor $k+1$ or $k+3$, depending on the direction of the electric field) after an additional drift time as illustrated in figure 7.

For the 'drift' injection, the exponential growth of the density is not allowed, in part in this case because the electric field becomes weaker by the time the particles (with density which has reached a 'final' value $n_f \gg n_{\rm th}$) are drifting out of their capacitor. The 'threshold' injection is assumed to take place before breakdown, and so the electric field is assumed to be strong throughout the (threshold injection) process.

Not only electrons are injected in both of the injection processes mentioned above, but also ions (to maintain the neutrality of the plasma). Even though in reality the electron cloud is slightly ahead of the ions, the error in the charge calculation due to injecting both is very small because the injected charge is too small to significantly change the electric field.

3.3. Acceleration of the simulation

Since breakdown of a cell is much faster than transport between cells, the discharge settles down between injection events, and this allows us to jump the simulation ahead to the next injection, after settling has occurred. We determine a 'settling time', $\tau_{\rm set}$, which is much larger than the characteristic time scale on which the density and fields relax, after an injection event. Then when the elapsed time since the last injection $\tau_{\rm el}$ obeys $\tau_{\rm el} \gtrsim \tau_{\rm set}$, we regard the simulated discharge as being in a quasi-equilibrium. No further changes are expected until the next injection event, so we are able to advance time (without integrating the equations) until the next injection time, when we begin integrating again, and so on. In practice, $\tau_{\rm set} \sim 0.6$ ns.

A time step is set to be $\Delta t = 0.05\tau_{\text{diel}}$ (where τ_{diel} is the dielectric relaxation time) which results in Δt being about 10^{-13} s. The total elapsed time for a run corresponds to approximately $(3 \times 10^8)\Delta t$. To illustrate the leap-ahead scheme, the first (threshold) injection happens at 0.9 ns. The next drift injection happens at 1.9 ns. After the previous injection we perform ∼5000 time steps in advancing the time by an amount τ_{set}. We then leap ahead by approximately 4×10^3 time steps. If there is one cell waiting to be injected, this leap-ahead scheme can save at least $(4 \times 10^3)\Delta t$ which is approximately 1 h on a Sun Blade 2000 (1.2 GHz UltraSPARC-III, 1 GB RAM) and the time saved scales in proportion with the number of injected cells. In general, injection events are separated by 50–100 times as long as the events described above, so the time saving is 50–100 times greater.

4. Simulation results

In this section, we discuss the results of the modelling to establish whether or not we can understand the behaviours obtained, since if we cannot we will conclude that the models are likely to be in error. It will be evident that the model presented above is the result of this process of testing and that the features discussed above were in part designed after earlier models proved less than satisfactory. A number of features of the model were required: the density does indeed move in a direction and at a speed which appears to be consistent with the electric field; the energy which is put into plasma formation is as expected, based on the stored energy in the electric field; plasma does not appear to form 'upstream' of where we believe it is energetically allowed to be. We begin with a more detailed examination of one particular simulation.

The plasma is formed from nitrogen gas (N_2) in a dielectric barrier discharge (5 mm gap between two 1.5 cm dielectric slabs with $\epsilon_r \sim 3.0$, at atmospheric pressure) with $\Delta x = 0.25$ mm (across the discharge gap) and $\Delta y = 6$ mm (along the electrodes which are 24 cm long). Details of the applied voltage are given next.

One of our objectives is to examine the effects of the nature of the applied voltage on the plasma which is formed. The middle part of the cathode (from $y = 8.4$ cm to 15.6 cm) in this example is biased with −75 kV, and the outer part ($y = 0$–8.4 cm and $y = 15.6$–24 cm) is biased with −7.5 kV (as shown in figure 8). The simulations are for N_2, where $\alpha \lesssim 0.1$. It is probably appropriate to compare the simulations with similar values of αV, so for inert gases with $\alpha \sim 1$ the applied voltage would be at least ten times smaller.

Since the plasma (including the surfaces where it is in contact with the dielectric) is overall charge neutral, the net flux of the electric field leaving it is zero. The plasma (being a good conductor) is at a potential V which is nearly constant in space. This potential must float in the middle of the range of values of the potential at the edges of the plasma, in order for the flux of electric field to be zero.

The time evolution of the breakdown is shown in figures 9 and 10. The complete potential profile (across the discharge and dielectric slabs) after the breakdown is shown in figure 11. A low initial electron density due to metastable neutral molecules at the dielectric surface exists on the left-hand side at the beginning of the cycle (the left-hand edge of the plasma shown in figure 9(*a*)). This density is assumed to be below threshold. The location at which this density reaches threshold, and at which threshold injection occurs, is approximately one cell to the right of where the group of electrons initially is. This threshold injection happens within 0.94 ns (not shown). After some time a denser neutral plasma is formed (in the cells where the density has reached threshold). The first drift injection starts from this neutral region, moving to the right-hand side of the discharge. Soon after the breakdown front has started moving in the x-direction, the plasma floating potential is lower than its surroundings

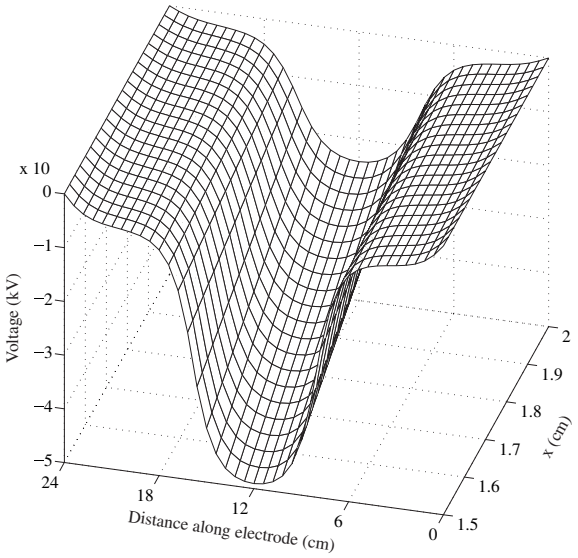

Figure 8. The vacuum potential. (The voltage within the dielectric slabs is not shown.)

at one end and at the other it is higher than its surroundings. Drift injection in the x-direction continues until the plasma reaches the dielectric surface on the right-hand side at time $\sim$50 ns. During breakdown, the floating potential gets higher. Electrons start to drift outwards in the $\pm y$-directions as the breakdown proceeds to the right-hand surface. (The injected density then spreads out in the x- and y-directions as shown. Injecting density into a cell where the electric field is too weak to cause breakdown, as opposed to where the density is too low, has very little effect because breakdown does not occur when the field drops below a critical value E_c, where E_c is approximately 10^5 V m^{-1}.)

As can be seen from the plots, the plasma does create a region where V is constant, which rapidly expands in x as the plasma expands. The feature of this region which is most interesting from the point of view of how the plasma evolves is the location of the point where E_y changes sign. Somewhere roughly halfway along the length of the plasma in the x-direction, E_y is expected to reverse. Electrons are pulled out in y at the right-hand side and pushed in on the left, in this example. However, as the plasma spreads in the x-direction, regions which were at first pulled out are later pushed back in.

As the breakdown proceeds in x, E_x (in front of and behind the plasma in the x-direction) increases leading to a higher density at the front of the plasma as it moves in x and a density peak at the right-hand side. As E_x inside the plasma becomes shielded out, the magnitude of E_x outside the plasma on the left-hand side gets bigger by a factor of 1.6. This is necessary to maintain the voltage dropped across the plasma. This also results in rapid growth of the electron peaks shown at the left-hand side of the discharge, as the strong E_x pushes the electrons at the left-hand side of the plasma further to the right.

A reversal of E_x at the right-hand surface of the discharge starts to develop at $t \simeq 0.22\ \mu$s (not shown). Electrons start to pile up on the right surface and some of the electrons in front of the surface are pulled out sideways (in the y-direction). Electrons which are injected in the y-direction have the potential to move in x and produce breakdown, although a sufficiently high E_x is needed if the breakdown is to continue in the x-direction at this y location. Since E_x gets weaker as the plasma moves outward in y (mostly because of the geometry employed),

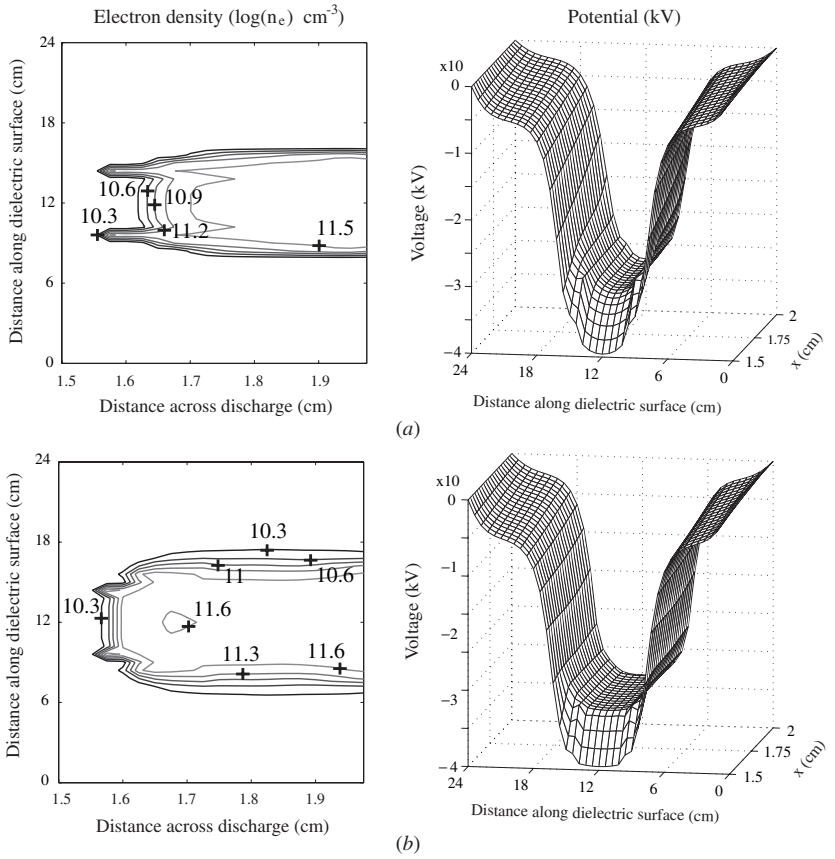

Figure 9. Time evolution of breakdown. The time evolution of electron density (on the left) and voltage in the discharge are shown. The contours in the density plots refer to the logarithm of the electron density per cubic centimetre. The outermost contour represents 2×10^{10} cm^{-3}. The electron density on the surfaces of the dielectric is not shown. Time = 58 ns (a) and 0.84 μs (b).

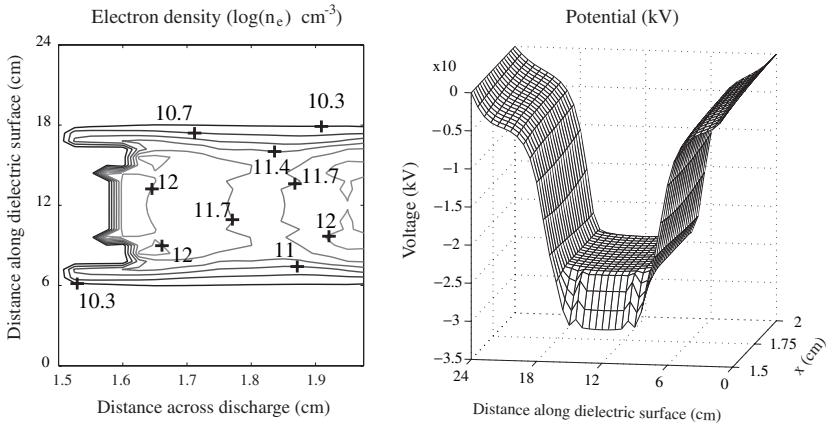

Figure 10. Time evolution of breakdown. The highest peak (during the observed time) has a magnitude of 2.3×10^{12} cm^{-3}. Time = 7.9 μs.

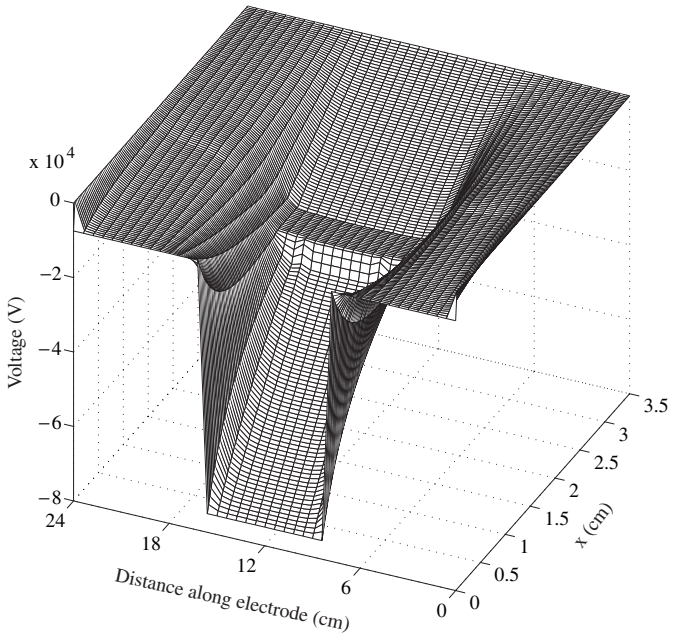

Figure 11. The voltage across the discharge and dielectric slabs at $t = 7.9\ \mu$s.

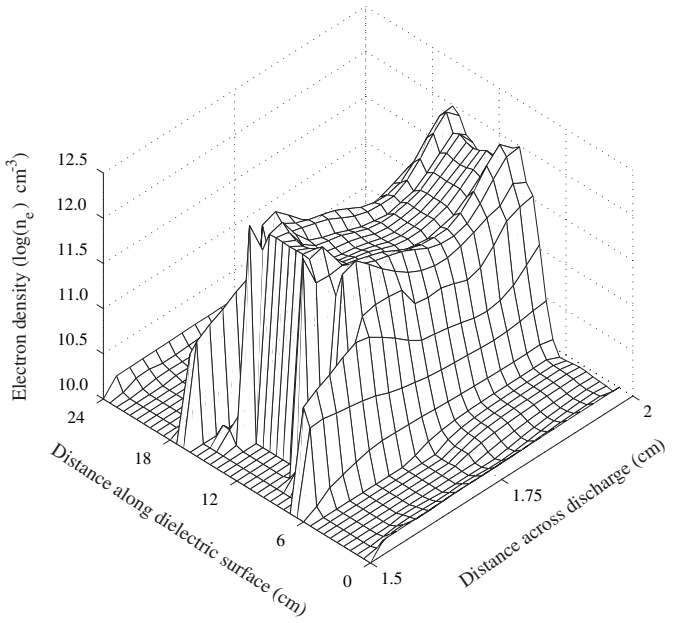

Figure 12. A perspective view of the logarithm of the electron density at 7.9 μs. $\Delta x = 0.25$ mm and $\Delta y = 6.0$ mm.

the breakdown will eventually stop spreading. Figure 12 shows a perspective view of the logarithm of the electron density at 7.9 μs. The best test of these results would be by means

of fully Lagrangian (mesh-free) 2D simulations [22]. We hope to develop such a calculation in future.

5. Conclusion

A method for simulation of breakdown in DBDs has been discussed, which is physically based and computationally efficient enough to allow multidimensional calculations. The key features of the method are that it results in very low levels of numerical diffusion and it captures the correct physics of the breakdown. Numerical diffusion can otherwise lead to density moving at the wrong rate and in the wrong direction; these problems are made severe by the extreme nature of breakdown. The other main issue addressed is ensuring that density only grows in a physically correct fashion, in accordance with conservation of energy. The main emphasis of this paper is on developing a model which reflects the physics which is believed to be taking place, and hence eliminating potential errors. A 'leap-ahead' scheme was outlined, which exploits the significant differences in time scale present in the problem to accelerate convergence.

Results of simulations were presented. Preliminary discussion of the physical principles controlling the breakdown process was given. It was argued that the models are behaving in a plausible fashion, since the main observations we can make are capable of being explained by means of simple arguments. While the accuracy of the model has been discussed in 1D [1], this has not been done yet in 2D. Future work will include Lagrangian (i.e. particle) simulations, which should allow us to test the validity of these models without sacrificing accuracy.

Appendix. Energy-conserving scheme

In this section, a fully energy-conserving scheme is described. The breakdown front has a number of electrons n_e which moves forward at a speed equal to $-\mu E$, giving rise to a flux per unit area per second of magnitude $n_e|\mu E|$. As the front advances, in the interval between two nodes, the number arriving at the 'target' node m per second (from node k) is thus

$$N_t = \frac{N_e[k]}{\Delta x}\,|\mu \boldsymbol{E}_{k-m}|\,\Delta t, \tag{A.1}$$

where $N_e[k]$ is the number of electrons at the source node k and $\mu \equiv \mu(E_{k-m})$. The number leaving the source node k is

$$N_s = N_t \exp\left(-\frac{\alpha}{\mathcal{E}_{\mathrm{iz}}} E \Delta x\right), \tag{A.2}$$

where $\alpha \equiv \alpha(E_{k-m})$. This gives the correct flux at the target node. It is clearly more physically correct than saying that equation (A.1) is the number leaving the source node, since if that were the case there would be an unphysically large flux at the target node. Thus, after moving electrons from node k to node m during one time step, the changes in electron numbers are

$$\Delta N_e[k] = -N_s \tag{A.3}$$

$$\Delta N_e[m] = N_t. \tag{A.4}$$

The number of ionizations is

$$\Delta N_{\mathrm{iz}} = N_t - N_s = N_t\left(1 - \exp\left(-\frac{\alpha}{\mathcal{E}_{\mathrm{iz}}} W_{k-m}\right)\right). \tag{A.5}$$

An ion charge ΔQ_i is introduced at each time step,

$$\Delta Q_i = q\Delta N_{\rm iz}. \tag{A.6}$$

The mean position $\bar{x}_i$ of the ions (measured from the node from which the electrons depart) can be written as

$$\begin{aligned}\bar{x}_i &= \frac{\int_0^{\Delta x} x\,{\rm e}^{\beta x}\,{\rm d}x}{\int_0^{\Delta x}{\rm e}^{\beta x}\,{\rm d}x}\\ &= \Delta x\frac{{\rm e}^{\beta\Delta x}}{{\rm e}^{\beta\Delta x}-1}-\frac{1}{\beta},\end{aligned} \tag{A.7}$$

where $\beta = \frac{\alpha E}{\mathcal{E}_{\rm iz}}$. If $\beta\Delta x \gg 1$, $\bar{x}_i \to \Delta x$; the ions will nearly all go to the target node. A simple convective scheme (CS) mapping rule [5] is used to share the positive charge (ΔQ_i) between the two nodes. Hence, when a number of electrons, $\Delta N_{\rm iz}$, are created while electrons are moving from node k to node m, the ion charge is shared between nodes k and m according to

$$\delta Q_i[k] = \left(1-\frac{\bar{x}_i}{\Delta x}\right)\Delta Q_i \tag{A.8}$$

$$\delta Q_i[m] = \frac{\bar{x}_i}{\Delta x}\Delta Q_i, \tag{A.9}$$

respectively. In this scheme, the electron charge Q_e and the ion charge Q_i are treated separately, unlike the previous description where the charge Q is the total charge.

In this version of the capacitor model, each capacitor in the network is no longer totally isolated. Once density is first injected into a capacitor (in the sense that the injection time has passed) all the negative fixed charge, Q_e, is converted to be mobile charge, qN_e. (The negative fixed charge Q_e at that node is set to be zero.) This results in a greater number of mobile charges being available for conduction than in the original scheme. The total charge Q at each node can be obtained by summing all the charges at the node, for example, the total charge at node k can be calculated from

$$Q[k] = \begin{cases} Q_i[k] + Q_e[k] & \text{if} \quad N_e[k] = 0.0 \text{ (before injection)},\\ Q_i[k] - qn_e[k] & \text{if} \quad N_e[k] > 0.0 \text{ (injection has occurred)}.\end{cases} \tag{A.10}$$

(Q_e is a negative number.) The voltage at each node is found as in equation (2).

References

[1] Wichaidit C and Hitchon W N G 2005 *Phys. Lett.* A **335** 50
[2] Hitchon W N G and Wichaidit C 2005 *J. Phys. A: Math. Gen.* **6841** 38
[3] Wichaidit C and Hitchon W N G 2005 *J. Comput. Phys.* **203** 650
[4] Kramer K and Hitchon W N G 1997 *Semiconductor Devices: A Simulation Approach* (Englewood Cliffs, NJ: Prentice-Hall)
[5] Hitchon W N G 1999 *Plasma Processes for Semiconductor Fabrication* (Cambridge: Cambridge University Press)
[6] Zhang P and Kortshagen U 2006 *J. Phys.* D **39** 153
[7] Carman R J, Mildren R P, Ward B K and Kane D M 2004 *J. Phys.* D **37** 2399
[8] Dhali S K and Williams P F 1985 *Phys. Rev.* A **31** 1219
[9] Yoshida K and Tagashira H 1976 *J. Phys.* D **9** 485
[10] Wu C and Kunhardt E E 1988 *Phys. Rev.* A **37** 4396
[11] Kulikovsky A A 1994 *J. Phys.* D **27** 2556
[12] Boeuf J P 1988 *J. Appl. Phys.* **63** 1342

[13] Li J and Dhali S K 1997 *J. Appl. Phys.* **82** 4205
[14] Barnes M S, Colter T J and Elta M E 1987 *J. Appl. Phys.* **61** 81
[15] Aleksandrov N L and Bazelyan E M 1996 *J. Phys.* D **29** 740
[16] Guo J M and Wu C J 1993 *J. Phys.* D **26** 487
[17] Guo J M and Wu C J 1993 *IEEE Trans. Plasma Sci.* **21** 684
[18] Kunhardt E E and Wu C 1987 *J. Phys.* D **68** 127
[19] Eastwood J W 1986 *Comput. Phys. Commun.* **43** 89
[20] Eastwood J W 1987 *Comput. Phys. Commun.* **44** 73
[21] Purser R J and Leslie L M 1994 *Mon. Weather Rev.* **122** 745
[22] Christlieb A J, Krasny R and Verboncoeur J P 2004 *IEEE. Trans. Plasma Sci.* **32** 384
[23] Parker G J, Hitchon W N G and Keiter E R 1996 *Phys. Rev.* E **54** 938
[24] Ashby D E T F 1980 private communication
[25] Morrow R and Blackburn T R 1999 *IEEE Trans. Plasma Sci.* **27** 26
[26] Kulikovsky A A 2000 *J. Phys.* D **33** 1514